⌘ *Author's Choice*

THE JOURNAL OF BIOLOGICAL CHEMISTRY VOL. 285, NO. 31, pp. 23954–23962, July 30, 2010

Multiple Palmitoyltransferases Are Required for Palmitoylation-dependent Regulation of Large Conductance Calcium- and Voltage-activated Potassium Channels*

Received for publication, April 24, 2010, and in revised form, May 26, 2010 Published, JBC Papers in Press, May 27, 2010, DOI 10.1074/jbc.M110.137802

Lijun Tian, Heather McClafferty, Owen Jeffries[1], and Michael J. Shipston[2]

From the Centre for Integrative Physiology, College of Medicine & Veterinary Medicine, University of Edinburgh, Edinburgh EH89XD, Scotland, United Kingdom

Palmitoylation is emerging as an important and dynamic regulator of ion channel function; however, the specificity with which the large family of acyl palmitoyltransferases (zinc finger Asp-His-His-Cys type-containing acyl palmitoyltransferase (DHHCs)) control channel palmitoylation is poorly understood. We have previously demonstrated that the alternatively spliced stress-regulated exon (STREX) variant of the intracellular C-terminal domain of the large conductance calcium- and voltage-activated potassium (BK) channels is palmitoylated and targets the STREX domain to the plasma membrane. Using a combined imaging, biochemical, and functional approach coupled with loss-of-function (small interfering RNA knockdown of endogenous DHHCs) and gain-of-function (overexpression of recombinant DHHCs) assays, we demonstrate that multiple DHHCs control palmitoylation of the C terminus of STREX channels, the association of the STREX domain with the plasma membrane, and functional channel regulation. Cysteine residues 12 and 13 within the STREX insert were the only endogenously palmitoylated residues in the entire C terminus of the STREX channel. Palmitoylation of this dicysteine motif was controlled by DHHCs 3, 5, 7, 9, and 17, although DHHC17 showed the greatest specificity for this site upon overexpression of the cognate DHHC. DHHCs that palmitoylated the channel also co-assembled with the channel in co-immunoprecipitation experiments, and knockdown of any of these DHHCs blocked regulation of the channel by protein kinase A-dependent phosphorylation. Taken together our data reveal that a subset of DHHCs controls STREX palmitoylation and function and suggest that DHHC17 may preferentially target cysteine-rich domains. Finally, our approach may prove useful in elucidating the specificity of DHHC palmitoylation of intracellular domains of other ion channels and transmembrane proteins.

S-Palmitoylation, the reversible addition of 16-carbon saturated palmitic acid to intracellular cysteine residues through a labile thioester linkage (1–5), is emerging as an important dynamic and potent determinant of ion channel function. Palmitoylation controls cell surface expression and regulation of many ligand-gated ion channels, including α-amino-3-hydroxyl-5-methyl-4-isoxazole-propionate (6), *N*-methyl-D-aspartate (7), Kainate (8), P2X7 (9), and γ-aminobutyric acid, type A (10–12). Palmitoylation also controls the function of voltage-gated calcium (13–15), sodium (16), and potassium (17–19) as well as other channels such as AQP4 (20). For example, in Kv1.1 potassium channels palmitoylation controls voltage dependence (18), and in the stress-regulated exon (STREX)[3] splice variant of large conductance calcium- and voltage-activated potassium (BK) channels, palmitoylation determines channel regulation by protein phosphorylation (19). However, although functional insights into ion channel regulation by protein palmitoylation are beginning to emerge, the control of channel palmitoylation is poorly understood, as for other palmitoylated proteins (21).

Protein palmitoylation is controlled by the balance of palmitoyl acyltransferases and palmitoyl thioesterases (1–5). Recently the zinc finger DHHC (Asp-His-His-Cys) type-containing protein family has emerged as a large family of palmitoyl acyltransferases with 23 members in the mouse and human genomes (22, 23). Previous studies have implicated the relatively promiscuous palmitoyltransferase DHHC3 (also known as Golgi-specific DHHC zinc finger protein, GODZ) in palmitoylating some ligand-gated ion channels (6, 7, 10, 12). However, the role of DHHC3 or other DHHCs in controlling palmitoylation of other ion channels, including BK channels, is not known. Furthermore, whether different DHHCs display specificity for palmitoylating individual ion channels has not been examined systematically. Elucidation of such DHHC-substrate relationships would provide significant insight into both the functional role of ion channel palmitoylation and the specificity of DHHCs for diverse target proteins.

We have previously demonstrated that a dicysteine motif (Cys^{12}-Cys^{13}) within the alternatively spliced STREX insert of the intracellular C terminus of BK channels (see Fig. 1) is palmitoylated and targets the C terminus to the plasma membrane in the absence of the transmembrane domains (19). In this manuscript, we have thus asked which DHHCs are responsible for palmitoylation of the STREX domain of the BK channel. We

* This work was supported by the Wellcome Trust.
⌘ *Author's Choice*—Final version full access.
[1] Recipient of a Biotechnology and Biological Sciences Research Council Ph.D. studentship.
[2] To whom correspondence should be addressed. Tel.: 44-131-6503253; Fax: 44-131-6506523; E-mail: mike.shipston@ed.ac.uk.

[3] The abbreviations used are: STREX, stress-regulated exon; BK channel, large conductance calcium- and voltage-activated potassium channel; DHHC, zinc finger Asp-His-His-Cys type-containing acyl palmitoyltransferase; HEK293, human embryonic kidney 293 cell; qRT, quantitative real time; siRNA, small interfering RNA; PKA, protein kinase A; PKAc, catalytic subunit of PKA; DMEM, Dulbecco's modified Eagle's medium; PBS, phosphate-buffered saline; HA, hemagglutinin; GFP, green fluorescent protein; YFP, yellow fluorescent protein; CRD, cysteine-rich domain.

took advantage of the robust endogenous palmitoylation of STREX channels in human embryonic kidney 293 (HEK293) cells as an assay system to systematically exploit both loss and gain of function approaches, through siRNA-mediated knockdown of endogenous DHHCs and overexpression of murine recombinant DHHCs, respectively, to interrogate the role of individual DHHCs in controlling STREX palmitoylation. In initial assays we exploited an imaging screen based on the palmitoylation-dependent plasma membrane localization of the intracellular STREX domain of the BK channel in HEK293 cells (19). Our data represent the first systematic analysis of the contribution of individual DHHCs in controlling palmitoylation of a voltage-gated ion channel. These studies reveal that multiple endogenous DHHCs control palmitoylation of STREX and that DHHC17 has the highest selectivity for the STREX Cys^{12}-Cys^{13} motif. Furthermore, we demonstrate that the DHHCs that regulate STREX palmitoylation can also assemble as a complex with the channel and determine the regulation of STREX channels by protein kinase A (PKA) phosphorylation.

EXPERIMENTAL PROCEDURES

Channel Constructs—The generation of full-length, C-terminal, and CRD epitope-tagged constructs of the STREX and ZERO variants of the murine BK channel has been described (19). All mutagenesis was performed using QuikChange mutagenesis (Stratagene) with constructs fully sequenced on both strands to verify sequence integrity.

Cell Culture, Transfection, and RNA Extraction—HEK293 cells were maintained in DMEM containing 10% fetal calf serum in a humidified atmosphere of 95% air, 5% CO_2 at 37 °C. The cells were passaged every 3–7 days using 0.25% trypsin in Hanks' buffered salt solution containing 0.1% EDTA. For RNA extraction or biochemical studies, the cells were grown in 24- or 6-well plates, respectively. For electrophysiological or imaging assays, the cells were plated on glass coverslips within 6-well plates. Twenty-four hours prior to the experiment, the cells were washed, and medium was replaced with DMEM containing ITS serum replacement (Sigma). The cells were transiently transfected at 40–60% confluence using Lipofectamine 2000 (Invitrogen) or FuGENE-HD (Roche Applied Science). For RNA interference, siRNAs were predesigned and supplied by Qiagen. The knockdown of DHHCs was performed in HEK293 cells by using two siRNAs (10–20 nM of each siRNA) for each gene. siRNA transfection was performed using HiperFect (Qiagen), essentially as described by the manufacturer. The respective cDNA was transfected 30 min after the completion of siRNA transfection. RNA extraction was carried out 48–72 h post-siRNA transfection using a High Pure RNA isolation kit (Roche Applied Science) according to the manufacturer's protocols. In all of the imaging and biochemical assays siRNA knockdown of DHHCs was monitored in parallel in each independent experiment. Independent experiments were conducted a minimum of three times in triplicate. The palmitoylation inhibitor 2-bromopalmitate (Sigma) was made as a fresh 100 mM stock in Me_2SO and applied at a final concentration of 100 μM overnight.

Quantitative Real Time PCR—cDNA was synthesized from the total mRNA of each DHHC knockdown sample using a Transcriptor High Fidelity cDNA synthesis kit (Roche Applied Science) as described by the manufacturer. The efficiency of knockdown of each DHHC at the mRNA level was analyzed using SYBR Green JumpStart Taq Ready Mix (Sigma) in a 25-μl total volume reaction on an ABIPrism 7000 real time PCR machine. Approximately 50–75 ng of cDNA was used per reaction with primers at 0.2 μM final concentrations. The internal reference control was endogenous β-actin detected using Qiagen primer set AT01680476. All of the reactions were performed in triplicate. Cycling conditions were 50 °C for 2 min, 95 °C for 10 min, followed by 40 cycles of 95 °C for 15 s, and then 60 °C for 1 min. All of the primers were previously validated with efficiencies calculated to be within 0.1 of the control using the equation $e = 10^{(1/\text{slope})} - 1$. The percentage of mRNA remaining was calculated using the equation % mRNA remaining $= 2^{-\Delta\Delta C_t} \times 100$.

Imaging—Briefly, the cells were plated on glass coverslips, transfected as above, and fixed 48 h after transfection except for experiments in Fig. 4 where cells were fixed 24 h post-transfection. The cells were first washed twice with PBS (Invitrogen) and then fixed with ice-cold 4% paraformaldehyde in PBS for 15 min at room temperature. The cells were washed three times with ice-cold PBS and quenched with 50 mM NH_4Cl in PBS for 10 min. The cells were washed three times in ice-cold PBS before mounting on microscope slides using Mowiol. The cells were initially analyzed under epifluorescence using an inverted Nikon Eclipse 2000 microscope using a 100× oil objective lens. High power confocal images were acquired on a Zeiss LSM510 laser scanning microscope, using a 63× oil Plan Apochromat (NA = 1.4) objective lens, in multi-tracking mode to minimize channel cross-talk. For each independent cell transfection, three or four coverslips/6-well cluster plate were analyzed for each construct. For each coverslip three to five random fields of view were analyzed to determine the number of transfected cells with plasma membrane localization of the respective fusion protein. The average percentage of transfected cells from each well was then determined for each independent transfection (experiment) and normalized to the corresponding wild type STREX control (membrane expression was typically observed in > 95% of transfected wild type STREX fusion proteins). The majority of experiments were performed blind. In addition, a random subset of cells was also analyzed by quantifying the relative peripheral membrane expression compared with the "intracellular" (cytoplasm + nucleus) expression using ImageJ. The ratio of membrane/intracellular fluorescence was determined and normalized to control treated cells assayed in the same experiment under identical conditions. There was no qualitative difference between these approaches. As such all of the data are expressed as percentages of the respective control means ± S.E. for N independent experiments, where n = minimum total number of cells analyzed across experiments for each construct/treatment.

Palmitoylation Assays, Pulldowns, and Western Blotting—CSS-palm prediction was performed using the published CSS-palm v2.0 palmitoylation algorithm (24).

[^{3}H]Palmitic Acid Incorporation—HEK293 cells were transiently transfected in 6-well cluster dishes (~ 3×10^6 cells/well) with the HA-tagged constructs as indicated in the respective figure legends. Forty-eight hours post-transfection, the cells were washed, and 1 ml of fresh DMEM containing 10 mg/ml

fatty acid free bovine serum albumin was added for 30 min at 37 °C. The cells were incubated in DMEM/bovine serum albumin containing 0.5 mCi/ml [^{3}H]palmitic acid (PerkinElmer Life Sciences) for 4 h at 37 °C, and then the medium containing the free label was removed. The cells were lysed in 150 mM NaCl, 50 mM Tris-Cl, 1% Triton X-100, pH 8.0, and centrifuged, and channel fusion proteins were captured using magnetic microbeads coupled to HA/GFP antibody (μMACS^{TM} epitope tag isolation kits; Miltenyi Biotech). After washing columns with 150 mM NaCl, 1% Nonidet P-40, 0.5% deoxycholate, 0.1% SDS, 50 mM Tris-Cl, pH 8.0, followed by washes with 50 mM Tris-Cl, pH 7.5, the captured proteins were eluted in SDS-PAGE sample buffer (50 mM Tris-Cl, pH 6.8, 5 mM dithiothreitol, 1% SDS, 1 mM EDTA, 0.005% bromphenol blue, 10% glycerol) prewarmed to 95 °C. The recovered samples were separated by SDS-PAGE, transferred to nitrocellulose membranes, and probed with either a monoclonal GFP antibody (Clontech; 1:3000) or polyclonal HA antibody (Zymed Laboratories Inc.; 1:1000). A duplicate membrane was dried and exposed to light-sensitive film at −80 °C using a Kodak Biomax transcreen LE (Amersham Biosciences). Co-immunoprecipitation experiments were performed essentially as described using the magnetic microbeads and antibodies as above.

Electrophysiological Assays—Single channel current recordings were performed in the inside-out configuration of the patch clamp technique at room temperature (20–24 °C). The pipette solution (extracellular) contained 140 mM NaCl, 5 mM KCl, 1 mM $CaCl_2$, 2 mM $MgCl_2$, 20 mM glucose, 10 mM HEPES, pH 7.4. The bath solution (intracellular) contained 140 mM KCl, 5 mM NaCl, 2 mM $MgCl_2$, 1 mM 1,2-bis(*o*-aminophenoxy)ethane-*N*,*N*,*N*′,*N*′-tetraacetic acid, 30 mM glucose, 10 mM HEPES, 1 mM ATP, pH 7.3, with free calcium $[Ca^{2+}]_i$ buffered to 0.1 μM, unless indicated otherwise. Channel activity was determined during 60-s depolarizations to +40 mV. Data acquisition and voltage protocols were controlled by an Axopatch 200B amplifier and pCLAMP9 software (Axon Instruments Inc., Foster City, CA). All of the recordings were sampled at 10 kHz and filtered at 2 kHz. Channel activity was allowed to stabilize for at least 10 min after patch excision before the addition of drugs. The catalytic subunit of PKA (PKAc) was from Promega (Madison, WI). Single-channel open probability (P_o) was derived from single-channel analysis using WINEDR (version 2.3.9; Dempster, J., University of Strathclyde, Strathclyde, UK). To determine the mean percentage of change in channel activity after a treatment, mean P_o or N^*P_o was measured immediately before and 10 min after the respective drug application. The effect of cAMP and/or PKAc on channel activity was typically maximal by ~5 min and remained stable over the next 10–30 min following application to inside-out patches. The effect of PKA-mediated phosphorylation was abolished in the absence of Mg-ATP and prevented using the PKA inhibitor PKI_{5-24} (data not shown and see Refs. 19 and 25–27).

Statistical Analysis—All of the data are presented as the means ± S.E. with N = number of independent experiments and n = number of individual cells analyzed in imaging assays. The data were analyzed by analysis of variance with post-hoc Dunnett's test or using a nonparametric Kruskal-Wallis test as appropriate with the significance set at $p < 0.05$.

RESULTS

Cysteine Residues within STREX Are the Only Endogenously Palmitoylated Residues in the Entire C Terminus of BK Channels—Expression of the entire intracellular C-terminal domain of the STREX splice variant of the murine BK channel as a HA- or GFP epitope-tagged construct (STREX-Cterm; Fig. 1*a*) in HEK293 cells resulted in robust palmitoylation (Fig. 1*b*) by endogenous palmitoyltransferases (DHHCs) and expression at the plasma membrane in the absence of the transmembrane domains (Fig. 1, *c* and *d*). We have previously demonstrated that the di-cysteine motif at amino acid positions 12 and 13 within the STREX insert is essential for this membrane localization and can be conferred by expression of the cysteine-rich domain (CRD) alone, which includes STREX and the immediately upstream heme-binding domain (19). In accordance with this, mutation of both cysteines to alanine (C12A/C13A) abolished palmitoylation of STREX-Cterm by endogenous DHHCs (Fig. 1*b*) as well as plasma membrane localization (Fig. 1*d*). In the C12A/C13A palmitoylation-deficient mutants, the fusion protein was robustly expressed as for wild type (Fig. 1*b*) but displayed a largely nuclear and/or cytoplasmic cellular distribution (Fig. 1*c*). Plasma membrane localization of the STREX C terminus, or CRD, was also abolished by preincubation of cells with the palmitoylation inhibitor 2-bromopalmitate (28, 29) (Fig. 1*d*). Furthermore, expression of the ZERO variant C terminus (ZERO-Cterm) that is identical to STREX-Cterm except with the exclusion of the STREX insert (19, 25, 27), was not palmitoylated by endogenous DHHCs in HEK293 cells and displayed a largely cytoplasmic distribution (Fig. 1, *b* and c). Taken together, these data demonstrate that the only cysteine residues within the entire C terminus of the STREX variant of the BK channel that are endogenously palmitoylated in HEK293 cells are cysteine residues 12 and 13 within the STREX insert.

Multiple Endogenous DHHCs Control Membrane Expression of the STREX Domain—In an attempt to address which DHHCs regulate palmitoylation of the STREX insert, we first examined the mRNA expression of endogenous DHHCs in our HEK293 cells. Using quantitative real time PCR (qRT-PCR) revealed expression of all 23 human DHHCs at the mRNA level (Fig. 2, *a* and *b*). In HEK293 cells DHHC4 mRNA was expressed at the highest level with most other DHHC mRNAs expressed at levels between 5 and 20% of DHHC4.

Based on this mRNA expression profile, we exploited multiple siRNAs against each DHHC isoform to allow us to screen the effect of knocking down DHHC isoforms on membrane localization of the STREX domain. For the majority of DHHCs, we could reliably achieve >80% knockdown (*i.e.* <20% mRNA remaining) of mRNA as determined by qRT-PCR, using two siRNAs/DHHC (Fig. 1*c*). In a few cases (*e.g.* DHHC 11 and 19), even using multiple distinct siRNA combinations, we were unable to achieve mRNA knockdown above 50%. Because antibodies are not available to reliably detect most DHHC isoforms, we were unable to monitor DHHC protein levels. Thus to monitor for knockdown efficiency in this system, we transfected siRNA against GFP to knock down expression of the STREX-Cterm-GFP fusion protein. Under our transfection conditions, typically >75% of all cells express the transfected fusion con-

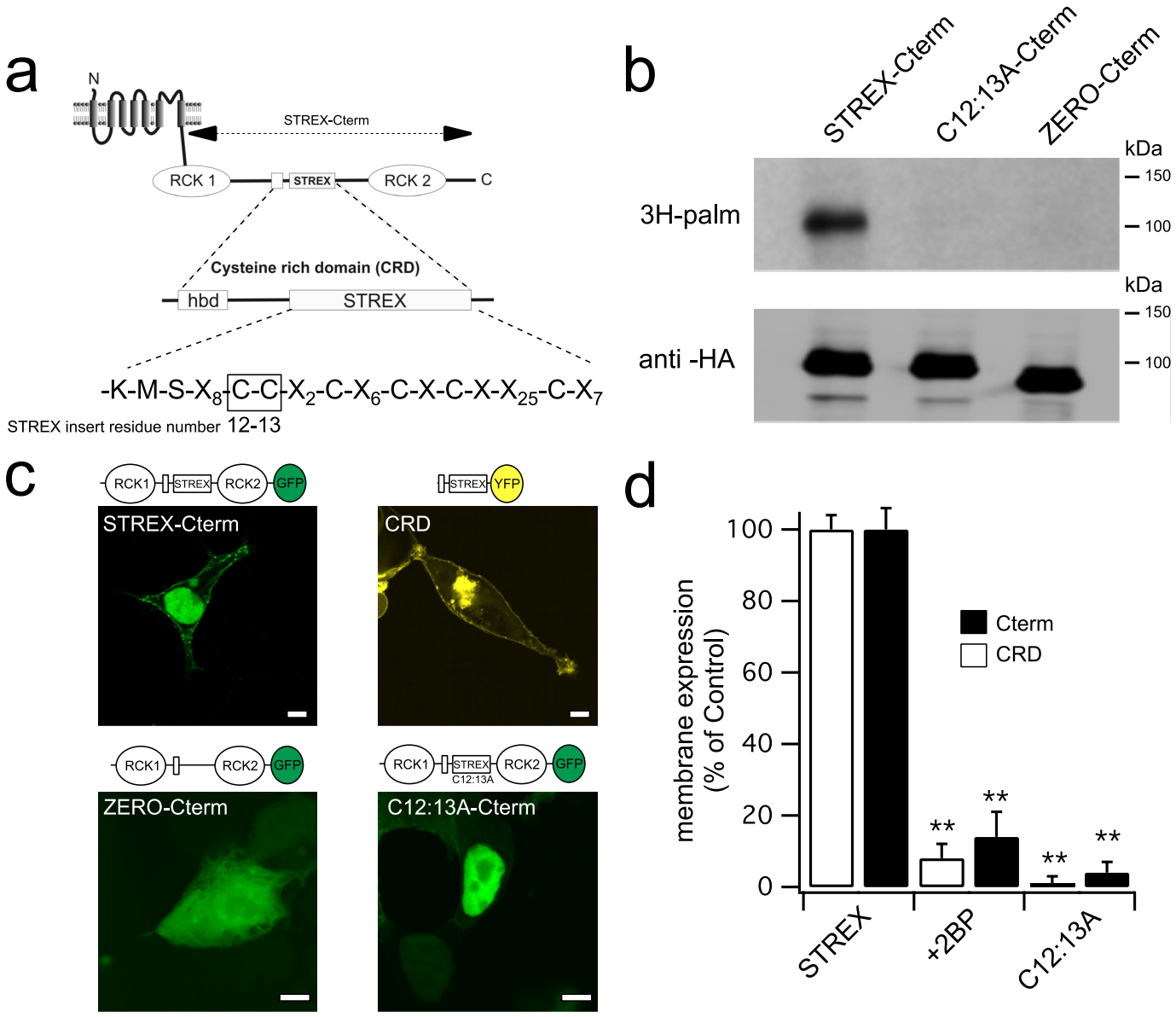

FIGURE 1. **Endogenous palmitoylation of the BK channel C terminus in HEK293 cells is only conferred by cysteine residues 12 and 13 in the alternatively spliced STREX insert.** *a*, schematic illustrating a single pore-forming α-subunit of the STREX splice variant of the BK channel. The STREX splice insert is localized in the intracellular linker between the two regulator of potassium conductance (RCK) domains. The STREX insert together with the upstream heme-binding domain represent the CRD of the linker. Amino acid numbering of the STREX insert starts with the first lysine residue, and cysteine residues 12 and 13 are predicted to be palmitoylated. *b*, fluorograph (*upper panel*) and corresponding Western blot (*lower panel*) of HA-tagged C-terminal constructs of the BK channel expressed in HEK293 cells. The cells were labeled with [^{3}H]palmitate (*3H-palm*) for 4 h, and the constructs were immunoprecipitated using anti-HA magnetic microbeads. *c*, representative single confocal sections and schematics of GFP C-terminal or YFP CRD constructs expressed in HEK293 cells. The *scale bars* are 5 μm. *d*, quantification of construct expression at the plasma membrane expressed as percentages of the membrane expression of the respective STREX-Cterm or CRD fusion protein. Cells treated with the palmitoyltransferase inhibitor 2-bromopalmitate (*2BP*) were exposed to 100 μM overnight. The data are the means $\pm$ S.E. where $N > 5$ and $n > 400$ for each construct/condition. **, $p < 0.01$, compared with respective STREX construct by analysis of variance with post-hoc Dunnett's test.

struct. In the presence of GFP siRNA, less than 2% of all cells displayed significant GFP expression, indicating that the efficiency of GFP knockdown was >97%.

By exploiting this siRNA screen in conjunction with expression of the CRD-YFP construct (to maximize signal/noise ratio), we first assayed the contribution of individual DHHCs to regulate the plasma membrane expression of the CRD-YFP construct in imaging assays. Individual knockdown of DHHCs 3, 5, 7, 9, and 17, but none of the other DHHCs in which high efficiency knockdown could be achieved resulted in a significant reduction in plasma membrane expression of the CRD-YFP fusion protein in HEK293 cells compared with the control (scrambled siRNA) alone (Fig. 2*d*), implicating these DHHCs in STREX palmitoylation. However, combinatorial knockdown of these DHHCs did not result in additive effects beyond those seen with the largest decrease in membrane expression of the CRD-YFP fusion protein with siRNA against DHHC9 (data not shown). Combinatorial knockdown was limited by the reduced efficiency of knockdown using multiple siRNAs and was limited by total siRNA concentrations >100 nM being toxic to cells. In contrast, inhibition of palmitoyltransferase activity using

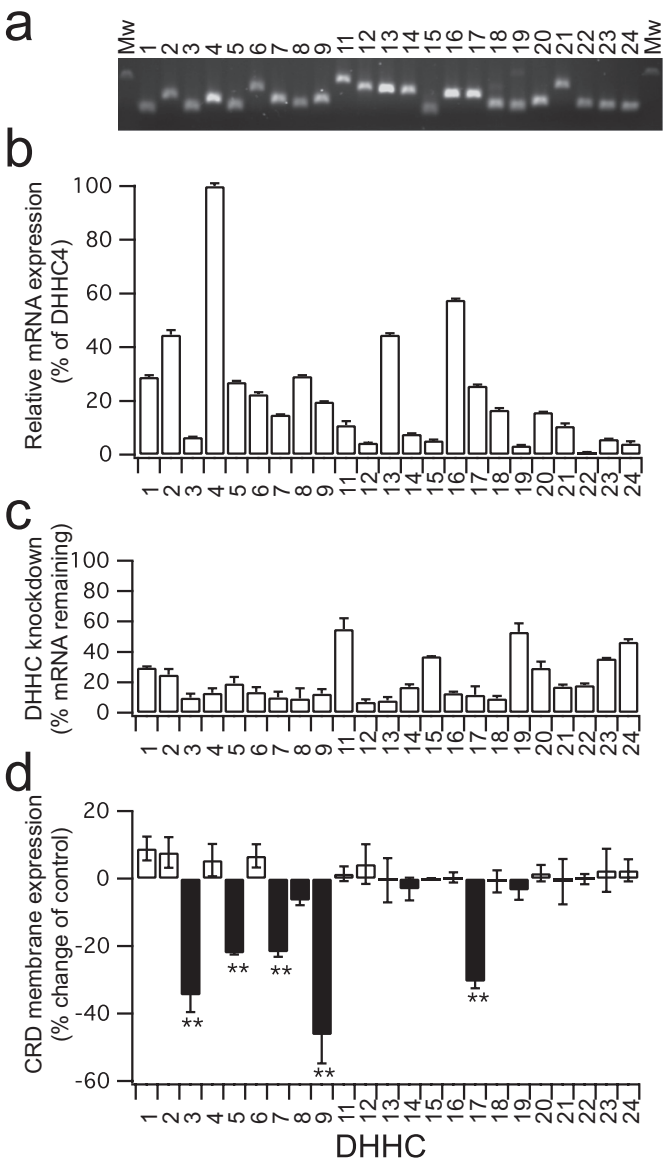

FIGURE 2. **Multiple endogenous DHHCs control membrane localization of the STREX domain.** *a*, representative agarose gel of Sybr-safe-stained PCR amplicons from real time qRT-PCR assays of DHHCs expressed in HEK293 cells (note numbering according to human DHHC convention, thus no DHHC10). *Mw*, molecular weight marker. *b*, relative mRNA expression of each DHHC expressed as a percentage of DHHC4. *c*, efficiency of siRNA-mediated knockdown of each DHHC using two independent siRNAs/DHHC. mRNA levels were quantified by qRT-PCR, and the mRNA expression remaining, following siRNA-mediated knockdown of the cognate DHHC, was expressed as a percentage of the respective control mRNA level for each DHHC. qRT-PCR assays were performed in parallel with the imaging assays in *d*. *d*, effect of DHHC knockdown on membrane expression of the CRD-YFP construct expressed in HEK293 cells. The data are expressed as the percentage of change in membrane expression compared with the CRD-YFP construct in the presence of the scrambled siRNA. The data are the means ± S.E. where $N > 3$ and $n > 350$ for each siRNA knockdown. **, $p < 0.01$, compared with CRD-YFP construct with scrambled siRNA by nonparametric Kruskal Wallis test with post-hoc test.

2-bromopalmitate reduced membrane expression of the CRD-YFP fusion protein to <10% of control (Fig. 1*d*).

Knockdown of DHHCs 3, 5, 7, 9, and 17 also significantly reduced plasma membrane expression of the STREX-Cterm-GFP fusion protein by ~50% (Fig. 3, *a* and *b*) compared with the scrambled siRNA control. To test whether siRNA knockdown of DHHCs 3, 5, 7, 9, and 17 in fact regulated palmitoylation status of the STREX domain, we assayed [^{3}H]palmitate incorporation into the STREX-Cterm construct. Importantly, siRNA knockdown of these DHHCs also significantly reduced but did not completely abolish palmitoylation of the STREX-Cterm fusion protein (Fig. 3, *c* and *d*). Similar reductions in both membrane expression and palmitoylation were observed when each individual DHHC was knocked down by siRNA. One possible explanation is that knockdown of any one of these DHHCs results in a compensatory reduction in expression of a common DHHC. For example, does knockdown of DHHC 3, 5, 7, or 9 also give a reduced DHHC17 expression? However, at least at the mRNA level, we saw no significant down-regulation of a common DHHC mRNA upon knocking down individual DHHCs (data not shown). Taken together these data suggest that the endogenous DHHCs 3, 5, 7, 9, and 17 are important determinants of the palmitoylation status of the STREX domain.

DHHC Overexpression Enhances Membrane Expression of the STREX C Terminus—If endogenous DHHCs 3, 5, 7, 9, and 17 control palmitoylation of the STREX domain, we hypothesized that overexpression of these DHHCs should enhance plasma membrane localization of the STREX C terminus. We thus co-expressed the STREX-Cterm-GFP construct with HA-tagged murine DHHCs (22) and examined the plasma membrane localization of STREX-Cterm-GFP in HEK-293 cells co-expressing both fusion proteins. To facilitate analysis we co-expressed constructs and imaged expression 24 h after expression. Under these conditions STREX-Cterm-GFP membrane localization is typically ~25% (Fig. 4*a*) of that seen under normal conditions when imaging is performed 48 h after transfection as in Figs. 1 and 3. Under these conditions, overexpression of DHHCs 3, 5, 7, 9, and 17 significantly increased (more than 2-fold) plasma membrane localization of the STREX-Cterm fusion protein (Fig. 4*b*). This stimulatory effect was not observed in the presence of the palmitoyltransferase inhibitor 2-bromopalmitate (data not shown).

In contrast, overexpression of DHHCs identified in our siRNA screen because not being involved in endogenous palmitoylation of the STREX domain, including those such as DHHCs 11, 19, and 24 in which siRNA knockdown was <70%, had no significant effect on STREX-Cterm-GFP expression at the plasma membrane (Fig. 4*c*). Furthermore, co-expression of the catalytically inactive palmitoyltransferase mutants DHHS3 or DHHS7 (22) had no effect on membrane expression, demonstrating that the palmitoyltransferase activity of the DHHCs is required rather than an effect via a possible chaperone function (Fig. 4*c*). To verify that the effect of DHHC overexpression was dependent upon palmitoylation of the STREX domain itself, we analyzed the effect of DHHCs 3, 5, 7, 9, and 17 on the C12A/C13A mutant of the STREX-Cterm fusion protein that is an absolute requirement for palmitoylation by endogenous DHHCs and expression at the plasma membrane (Fig. 1, *b*–*d*). Under these conditions membrane expression of the C12A/C13A fusion alone is almost undetectable (Fig. 4*d*). Surprisingly, overexpression of DHHCs 3, 5, 7, or 9 also significantly enhanced membrane expression of the C12A/C13A fusion protein to levels that in fact approached that observed upon co-expression with the wild-type STREX-Cterm-GFP (Fig. 4*d*). In contrast, although there was a small effect of DHHC17 to

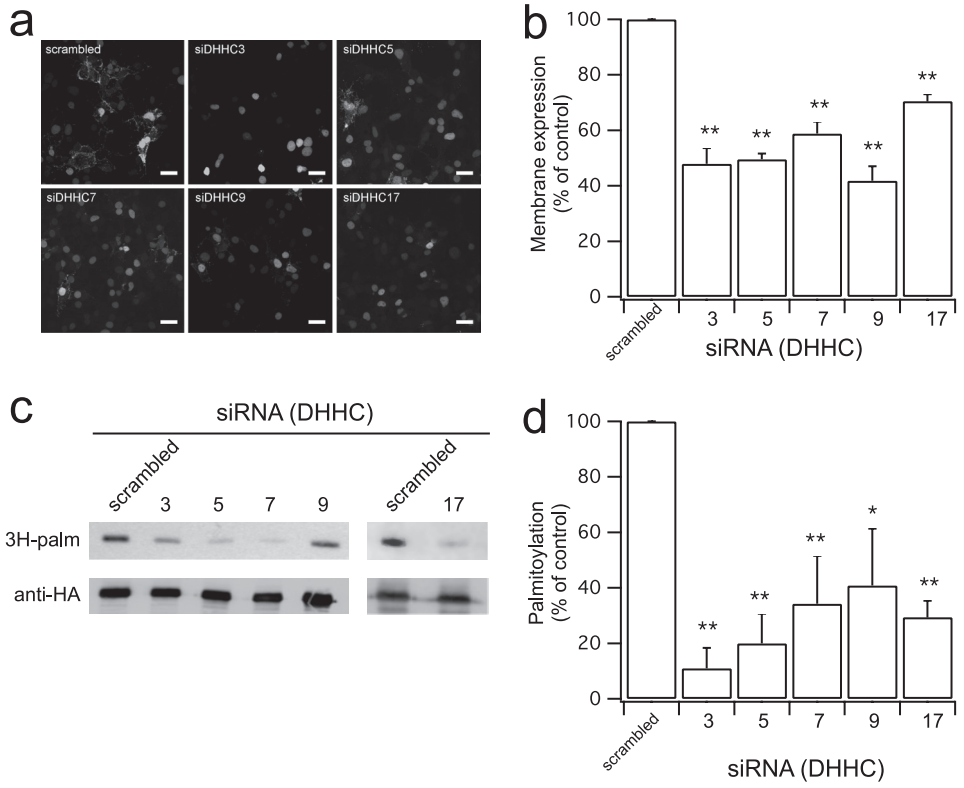

FIGURE 3. **DHHCs 3, 5, 7, 9, and 17 control STREX palmitoylation and membrane association.** *a*, representative low power confocal sections of HEK293 cells expressing the STREX-Cterm-GFP fusion protein and transfected with siRNA against the indicated DHHC. The *scale bars* are 20 μm. *b*, quantification of STREX-Cterm-GFP membrane localization, expressed as a percentage of the membrane localization with the scrambled siRNA, following the respective DHHC knockdown. The data are the means ± S.E. where $N > 4$ and $n > 350$ for each siRNA knockdown. *c*, fluorograph (*upper panel*) and corresponding Western blot (*lower panel*) of HA-tagged C-terminal constructs of the BK channel expressed in HEK293 cells. The cells were labeled with [^{3}H]palmitate (*3H-palm*) for 4 h, and the constructs were immunoprecipitated using anti-HA magnetic microbeads. *d*, quantification of STREX-Cterm palmitoylation following siRNA knockdown of DHHCs by siRNA as in *c*. The data are expressed as percentages of palmitate incorporation in the STREX-Cterm construct in scrambled siRNA-treated cells. The data are the means ± S.E., $N = 3–4$. *, $p < 0.05$; **, $p < 0.01$, compared with respective scrambled control group by analysis of variance with post-hoc Dunnett's test.

increase membrane expression of the C12A/C13A mutant, expression was still significantly lower (<40%) than that seen with the STREX-Cterm alone. These data imply that DHHC 17 is likely the most selective DHHC for palmitoylation of cysteines 12 and 13 in the STREX domain but also suggest that additional palmitoylation sites can be engaged by overexpression of DHHCs to control membrane expression of the C terminus of the STREX BK channel.

Intriguingly, the cysteine residue (Cys^{16}) immediately downstream of cysteines 12 and 13 within the STREX domain is also predicted to be palmitoylated using the CSS-PALM v2.0 algorithm (24). To address whether Cys^{16} may be a target for overexpressed DHHCs, we made the triple mutant C12A/C13A/C16A, in which all three cysteines are mutated to alanine. The construct was robustly expressed in HEK293 cells but failed to be located at the plasma membrane as predicted (Fig. 4*e*). However, co-expression of any DHHC now failed to enhance plasma membrane localization of the C12A/C13A/C16A construct (Fig. 4*e*). Taken together, these data suggest that DHHC17 is most selective for cysteines 12 and 13 within STREX but that exogenous overexpression of DHHCs 3, 5, 7, or 9 can also regulate palmitoylation status and membrane localization via Cys^{16}.

DHHCs Co-immunoprecipitate with STREX BK Channels—Previous studies have suggested that a number of palmitoylated proteins can assemble with their cognate DHHCs (2, 12, 21, 30). Because multiple DHHCs are able to control the palmitoylation status of the STREX domain, we asked whether DHHCs may be able to assemble in a complex with the full-length BK channel. In these studies full-length STREX channels with a C-terminal GFP fusion were co-expressed with HA-tagged DHHCs in HEK293 cells and subjected to reciprocal co-immunoprecipitation assays. Pulldown using anti-HA antibodies resulted in robust immunoprecipitation of DHHCs 3, 5, 7, 9, and 17. Immunoprecipitates were probed for the GFP tag on the BK channel, revealing co-immunoprecipitation with each DHHC (Fig. 5*a*). Immunoprecipitation controls including cells expressing STREX-GFP channel alone (Fig. 5, *control*) or beads alone (not shown) did not result in co-immunoprecipitation. Similar results were observed with the reciprocal pulldown in which channels were immunoprecipitated with anti-GFP and probing for the HA tag on the respective GFP (Fig. 5*b*), except that under these conditions we could not reliably co-immunoprecipitate DHHC5.

Knockdown of DHHC3, 5, 7, 9, or 17 Prevents PKA-mediated Inhibition of the STREX Channel—To address the functional relevance of STREX domain palmitoylation controlled by DHHC3, 5, 7, 9, and 17, we examined the functional cross-talk between the palmitoylation and PKA-dependent phosphorylation of the STREX channel reported previously (19). Phosphorylation of the STREX domain by PKA leads to channel inhibition; however, this inhibition is conditional on the STREX domain being palmitoylated and associated with the plasma membrane (19).

In cells treated with the scrambled siRNA, application of cAMP to the intracellular face of inside-out patches from HEK293 cells expressing the full-length STREX channel resulted in robust inhibition of STREX channel activity that is entirely dependent upon endogenous PKA activity closely associated with the channel (19, 25, 27), as reported previously in control conditions (Fig. 6). However, in cells in which DHHCs 3, 5, 7, 9, or 17 were individually knocked down by siRNA, cAMP-mediated inhibition of the channel was completely abolished (Fig. 6). To validate that the lack of cAMP-mediated inhibition of STREX channel activity in cells in which these DHHCs have been knocked down does not result from disruption of cAMP-dependent activation of PKA, we also analyzed the effect of applying the PKAc to the intracellular face of the patch. Under these conditions application of PKAc in control siRNA

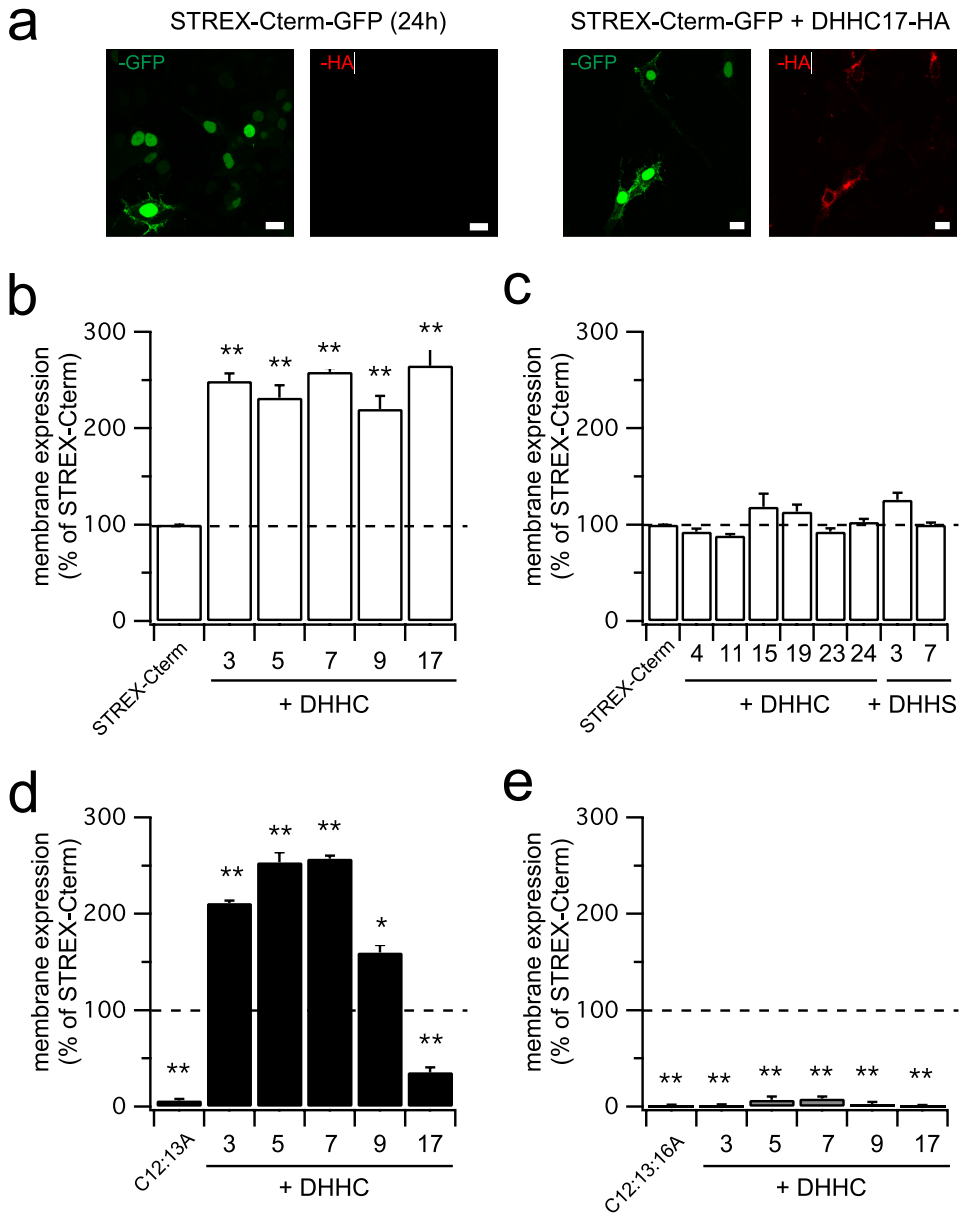

FIGURE 4. **DHHC overexpression enhances membrane localization of STREX-Cterm.** *a*, representative low power confocal sections of HEK293 cells 24 h after transfection with STREX-Cterm-GFP (*left-hand panels*) or co-transfected with DHHC17 (*right-hand panels*). Under each condition the STREX-Cterm-GFP localization and HA tag image planes are shown. The *scale bars* are 10 μm. *b* and *c*, quantification of STREX-Cterm-GFP. *d* and *e*, C12A/C13A (*d*) and C12A/C13A/C16A (*e*) membrane localization in cells co-expressing the corresponding DHHC, or the inactive mutant (DHHS). In *b–e*, the data are expressed as percentages of STREX-Cterm-GFP membrane localization observed in the absence of overexpressed palmitoyltransferase (100%, *dashed line*). The data are the means ± S.E. where $N > 5$ and $n > 400$ for each group. *, p 0.05; **, $p < 0.01$, compared with the STREX-Cterm-GFP construct in the absence of overexpressed palmitoyltransferase by analysis of variance with post-hoc Dunnett's test.

transfected cells inhibited STREX channel activity by 68 ± 8%, $n = 7$. In contrast, in cells in which DHHC17 was knocked down by siRNA, no significant change in activity was observed (mean change in activity was 10.8 ± 8.3%, $n = 5$). Thus knockdown of any of the DHHCs implicated in regulating palmitoylation of the STREX domain also controls the regulation of STREX channels by PKA-mediated phosphorylation.

DISCUSSION

Our data provide the first systematic analysis of the role of individual DHHC palmitoyltransferases in the palmitoylation and regulation of a voltage-gated ion channel. We demonstrate that the intracellular alternatively spliced STREX domain of BK channels is endogenously palmitoylated by multiple palmitoyltransferases (DHHCs). Using siRNA knockdown, DHHCs 3, 5, 7, 9, and 17 were all shown to control STREX domain palmitoylation and association of the STREX C terminus with the plasma membrane. Importantly, knockdown of these DHHCs also controlled PKA-dependent inhibition of the STREX BK channel that we have previously shown to be the major functional effect of palmitoylation of STREX in BK channels (19).

Previous analysis of ligand-gated ion channels has revealed an important role for DHHC3 (also known as GODZ) in controlling channel palmitoylation (6, 7, 10, 12, 30). DHHC3 is rather promiscuous in its palmitoylation of target proteins (21, 22, 31), and DHHC3 controlled palmitoylation of STREX. DHHC7, which may heteromultimerize with DHHC3 (10), was also implicated in STREX palmitoylation. In addition DHHC9, DHHC5, and DHHC17 also controlled STREX palmitoylation and function. The regulation of STREX by DHHC17 is particularly intriguing because DHHC17 is also reported to palmitoylate other cysteine-rich proteins including SNAP25 (32), cysteine string protein (33), and huntingtin (34). Overexpression assays suggested that DHHC17 has the highest selectivity for the palmitoylated dicysteine motif of STREX (cysteines 12 and 13 in STREX). Taken together, because Cys^{12}-Cys^{13} falls within a cysteine-rich domain, as a result of inclusion of the alternatively spliced STREX exon, this may suggest that DHHC17 may preferentially palmitoylate cysteine residues within internal cysteine-rich domains of proteins.

The ability of multiple DHHCs to target the same protein appears to be a general recurring theme in protein palmitoylation. However, it is somewhat surprising that knockdown of any one of these DHHCs (3, 5, 7, 9 or 17) has very similar effects on palmitoylation status, membrane association, and the ability to prevent PKA-mediated inhibition of STREX channels. Indeed, although our attempts to simultaneously knock down all of these DHHCs was unsuccessful, there was no significant addi-

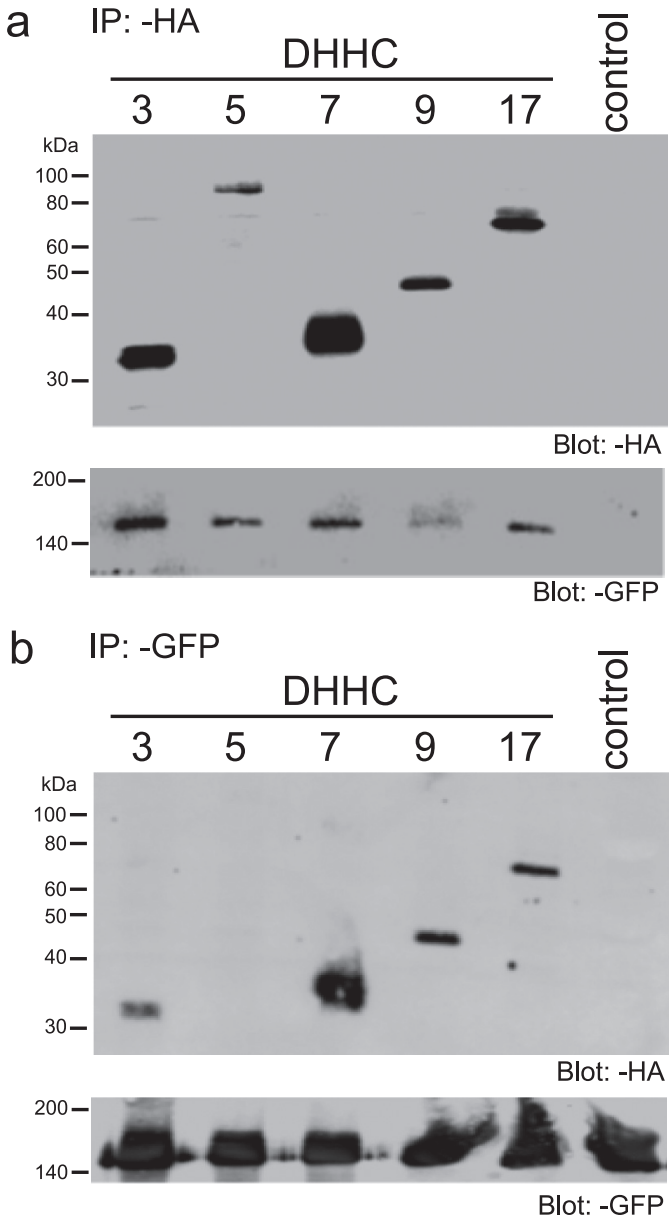

FIGURE 5. **DHHCs 3, 5, 7, 9, and 17 co-immunoprecipitate with full-length STREX BK channel.** Western blots of co-immunoprecipitated HA-tagged DHHCs with GFP-tagged full-length STREX BK channels expressed in HEK293 cells. In *a*, DHHCs were immunoprecipitated (*IP*) with anti-HA magnetic microbeads, and in *b*, channels were immunoprecipitated using anti-GFP magnetic microbeads, and immunoprecipitates were subjected to SDS-PAGE and transferred to polyvinylidene difluoride. The immobilon and the respective tag were probed and detected by enhanced chemiluminescence.

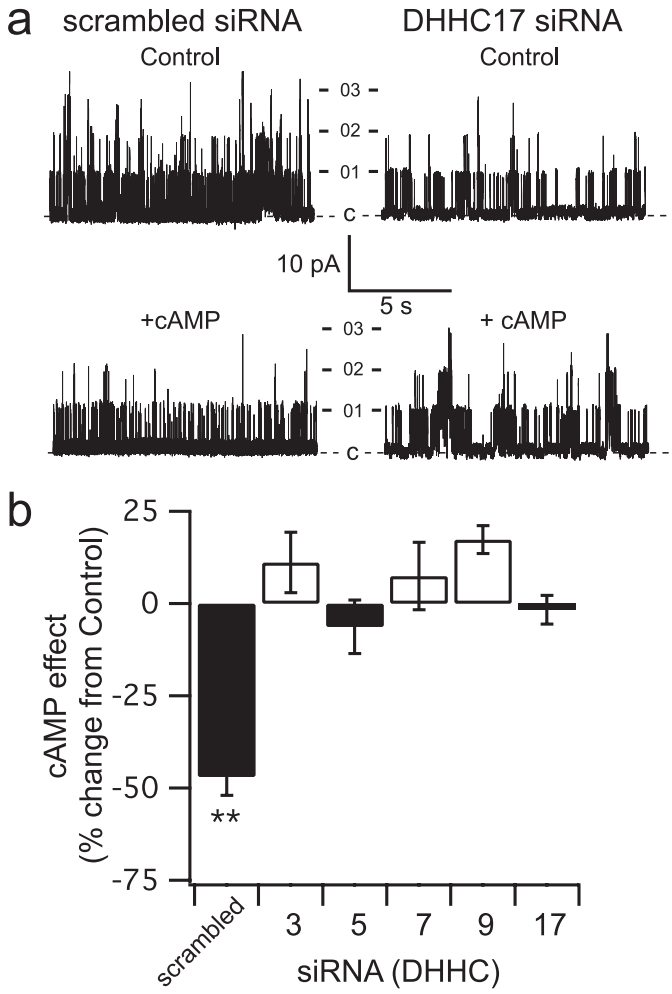

FIGURE 6. **DHHC knockdown prevents PKA-mediated inhibition of STREX channels.** *a*, representative single channel traces from excised inside-out patches of HEK293 cells expressing full-length STREX BK channels before and 5 min after exposure to cAMP. *Left-* and *right-hand panels* are from cells co-transfected with scrambled and DHHC17 siRNA, respectively. Patches were held at +40 mV in physiological potassium gradients with intracellular free calcium buffered to 0.1 μM in the presence of 2 mM Mg-ATP. *b*, summary bar chart of the effect of cAMP on STREX single channel open probability (P_o) expressed as the percentage of change in activity from pre-cAMP control under each condition. The data are the means ± S.E., $N = 6–10$/group. **, $p < 0.01$, compared with the scrambled siRNA group by nonparametric Kruskal Wallis test with post-hoc test.

tive effect on multiplexing siRNA knockdown. Multiple distinct mechanisms may be involved in this effect, resulting in each DHHC having an effect in controlling palmitoylation and function, as has been suggested with other proteins. For example, it may simply reflect that the normal cellular expression of each of these DHHCs is required for efficient palmitoylation as the channel traffics to the plasma membrane. It may also reflect potential different localization of specific DHHC substrate interactions occurring within the trafficking pathway. This may be particularly important for tetrameric proteins like BK channels such that a combinatorial code of palmitoylation on multiple sites across multiple subunits is important for the overall palmitoylation status and functional effect. For example, eight cysteine residues (*i.e.* 4× Cys^{12} and Cys^{13} in STREX) would be available for palmitoylation in the tetrameric homomeric channel. Although the majority of DHHCs that control STREX palmitoylation are thought to be Golgi/endoplasmic reticulum-localized upon overexpression (23), the localization of endogenous DHHCs and their potential trafficking is poorly understood because of the lack of available antibodies to characterize many of the endogenous DHHC proteins. Additional mechanisms may also exist. As already discussed, heteromultimerization of DHHCs may occur as previously demonstrated using overexpressed DHHC3 and DHHC7 (10), or the activity/localization of DHHCs may themselves be controlled by palmitoylation as has been shown for autopalmitoylation of some DHHCs (2). However, the extent to which other DHHCs heteromultimerize, the role of heteromultimerization, and the

functional effect of DHHC palmitoylation in native systems are largely unknown.

An additional factor that may also be important is the stoichiometry of BK channel palmitoylation that is required for the functional effects of palmitoylation to be manifest. In this regard, we have previously shown that phosphorylation of only a single STREX domain in the channel tetramer is important for functional regulation (25). Whether this is also the case for palmitoylation remains to be determined.

Increasing evidence suggests that DHHCs may assemble with their target substrates. For example, DHHC3 and 17 assemble with SNAP25 (21), whereas DHHC3 has been shown to form a complex with γ-aminobutyric acid, type A and α-amino-3-hydroxyl-5-methyl-4-isoxazole-propionate receptors (12, 30). Our data reveal that, at least in overexpression systems, the cognate DHHCs that palmitoylate the STREX domain also can assemble as a complex with the channel. Clearly whether the interaction is direct or results from assembly as a much larger macromolecular complex in native systems warrants further investigation. Furthermore, whether cycles of palmitoylation/depalmitoylation are required as the channels traverse different stages in the pathway leading to delivery to the cell surface remains to be explored.

Intriguingly, overexpression of DHHCs that endogenously control STREX palmitoylation (apart from DHHC17) also allowed access of these DHHCs to a cysteine residue (Cys^{16}) immediately downstream of the Cys^{12}-Cys^{13} site. This implies that Cys^{16} may also be a target for palmitoylation in some cell types in which these DHHCs have access to the site, thus extending the potential repertoire by which STREX channels may be regulated by palmitoylation. However, no other cysteine residues within the entire C terminus of the channel were targets for palmitoylation in HEK293 cells because mutation of Cys^{12}-Cys^{13} completely abolished palmitate incorporation by endogenous DHHCs.

In conclusion, our work reveals that DHHCs 3, 5, 7, 9, and 17 are important determinants of STREX BK channel palmitoylation, STREX domain interaction with the plasma membrane, and functional regulation. Our approach thus represents the first systematic analysis of ion channel palmitoylation by the multimember DHHC family of palmitoyltransferases. Our strategy employing both loss and gain of function strategies and utilizing fluorescent fusion proteins to screen for the effects of palmitoylation of plasma membrane expression of palmitoylated domains of transmembrane proteins may serve as an approach to further interrogate the specificity and role of DHHCs in controlling ion channel and other plasma membrane transmembrane protein regulation by protein palmitoylation.

Acknowledgments—We are grateful to Dr. Trudi Gillespie (IMPACT imaging facility, Centre for Integrative Physiology) for assistance in confocal imaging. We are grateful to Dr. Masaki Fukata for the generous gifts of the murine DHHC constructs and Dr. Luke Chamberlain for advice and DHHS3 and 7 constructs.

REFERENCES

1. el-Husseini, Ael-D, and Bredt, D. S. (2002) *Nat. Rev. Neurosci.* **3,** 791–802
2. Fukata, Y., and Fukata, M. (2010) *Nat. Rev. Neurosci.* **11,** 161–175
3. Kang, R., Wan, J., Arstikaitis, P., Takahashi, H., Huang, K., Bailey, A. O., Thompson, J. X., Roth, A. F., Drisdel, R. C., Mastro, R., Green, W. N., Yates, J. R., 3rd, Davis, N. G., and El-Husseini, A. (2008) *Nature* **456,** 904–909
4. Linder, M. E., and Deschenes, R. J. (2007) *Nat. Rev. Mol. Cell Biol.* **8,** 74–84
5. Resh, M. D. (2006) *Nat. Chem. Biol.* **2,** 584–590
6. Hayashi, T., Rumbaugh, G., and Huganir, R. L. (2005) *Neuron* **47,** 709–723
7. Hayashi, T., Thomas, G. M., and Huganir, R. L. (2009) *Neuron* **64,** 213–226
8. Pickering, D. S., Taverna, F. A., Salter, M. W., and Hampson, D. R. (1995) *Proc. Natl. Acad. Sci. U.S.A.* **92,** 12090–12094
9. Gonnord, P., Delarasse, C., Auger, R., Benihoud, K., Prigent, M., Cuif, M. H., Lamaze, C., and Kanellopoulos, J. M. (2009) *FASEB J.* **23,** 795–805
10. Fang, C., Deng, L., Keller, C. A., Fukata, M., Fukata, Y., Chen, G., and Lüscher, B. (2006) *J. Neurosci.* **26,** 12758–12768
11. Rathenberg, J., Kittler, J. T., and Moss, S. J. (2004) *Mol. Cell Neurosci.* **26,** 251–257
12. Keller, C. A., Yuan, X., Panzanelli, P., Martin, M. L., Alldred, M., Sassoè-Pognetto, M., and Lüscher, B. (2004) *J. Neurosci.* **24,** 5881–5891
13. Chan, A. W., Owens, S., Tung, C., and Stanley, E. F. (2007) *Cell Calcium* **42,** 419–425
14. Chien, A. J., Carr, K. M., Shirokov, R. E., Rios, E., and Hosey, M. M. (1996) *J. Biol. Chem.* **271,** 26465–26468
15. Hurley, J. H., Cahill, A. L., Currie, K. P., and Fox, A. P. (2000) *Proc. Natl. Acad. Sci. U.S.A.* **97,** 9293–9298
16. Schmidt, J. W., and Catterall, W. A. (1987) *J. Biol. Chem.* **262,** 13713–13723
17. Jindal, H. K., Folco, E. J., Liu, G. X., and Koren, G. (2008) *Am. J. Physiol.* **294,** H2012–H2021
18. Gubitosi-Klug, R. A., Mancuso, D. J., and Gross, R. W. (2005) *Proc. Natl. Acad. Sci. U.S.A.* **102,** 5964–5968
19. Tian, L., Jeffries, O., McClafferty, H., Molyvdas, A., Rowe, I. C., Saleem, F., Chen, L., Greaves, J., Chamberlain, L. H., Knaus, H. G., Ruth, P., and Shipston, M. J. (2008) *Proc. Natl. Acad. Sci. U.S.A.* **105,** 21006–21011
20. Suzuki, H., Nishikawa, K., Hiroaki, Y., and Fujiyoshi, Y. (2008) *Biochim. Biophys. Acta* **1778,** 1181–1189
21. Huang, K., Sanders, S., Singaraja, R., Orban, P., Cijsouw, T., Arstikaitis, P., Yanai, A., Hayden, M. R., and El-Husseini, A. (2009) *FASEB J.* **23,** 2605–2615
22. Fukata, M., Fukata, Y., Adesnik, H., Nicoll, R. A., and Bredt, D. S. (2004) *Neuron* **44,** 987–996
23. Ohno, Y., Kihara, A., Sano, T., and Igarashi, Y. (2006) *Biochim. Biophys. Acta* **1761,** 474–483
24. Ren, J., Wen, L., Gao, X., Jin, C., Xue, Y., and Yao, X. (2008) *Protein Eng. Des. Sel.* **21,** 639–644
25. Tian, L., Coghill, L. S., McClafferty, H., MacDonald, S. H., Antoni, F. A., Ruth, P., Knaus, H. G., and Shipston, M. J. (2004) *Proc. Natl. Acad. Sci. U.S.A.* **101,** 11897–11902
26. Tian, L., Coghill, L. S., MacDonald, S. H., Armstrong, D. L., and Shipston, M. J. (2003) *J. Biol. Chem.* **278,** 8669–8677
27. Tian, L., Duncan, R. R., Hammond, M. S., Coghill, L. S., Wen, H., Rusinova, R., Clark, A. G., Levitan, I. B., and Shipston, M. J. (2001) *J. Biol. Chem.* **276,** 7717–7720
28. Jennings, B. C., Nadolski, M. J., Ling, Y., Baker, M. B., Harrison, M. L., Deschenes, R. J., and Linder, M. E. (2009) *J. Lipid Res.* **50,** 233–242
29. Resh, M. D. (2006) *Methods* **40,** 191–197
30. Uemura, T., Mori, H., and Mishina, M. (2002) *Biochem. Biophys. Res. Commun.* **296,** 492–496
31. Fukata, Y., Iwanaga, T., and Fukata, M. (2006) *Methods* **40,** 177–182
32. Greaves, J., Prescott, G., Fukata, Y., Fukata, M., Salaun, C., and Chamberlain, L. (2009) *Mol. Biol. Cell* **20,** 1845–1854
33. Greaves, J., Salaun, C., Fukata, Y., Fukata, M., and Chamberlain, L. H. (2008) *J. Biol. Chem.* **283,** 25014–25026
34. Yanai, A., Huang, K., Kang, R., Singaraja, R. R., Arstikaitis, P., Gan, L., Orban, P. C., Mullard, A., Cowan, C. M., Raymond, L. A., Drisdel, R. C., Green, W. N., Ravikumar, B., Rubinsztein, D. C., El-Husseini, A., and Hayden, M. R. (2006) *Nat. Neurosci.* **9,** 824–831